

The Nature of Millisecond Pulsars with Helium White Dwarf Companions

Sarah L. Smedley¹, Christopher A. Tout^{1,2,3}, Lilia Ferrario³

and Dayal T. Wickramasinghe³

¹ *Institute of Astronomy, The Observatories, Madingley Road, Cambridge, CB3 0HA*

² *Monash Centre for Astrophysics, School of Mathematics, Building 28, Monash University, Clayton, VIC 3800, Australia*

³ *Mathematical Sciences Institute, The Australian National University, ACT 0200, Australia*

Accepted. 2013 October 21 Received 2013 October 16; in original form 2012 December 21

ABSTRACT

We examine the growing data set of binary millisecond pulsars that are thought to have a helium white dwarf companion. These systems are believed to form when a low-to intermediate-mass companion to a neutron star fills its Roche lobe between central hydrogen exhaustion and core helium ignition. We confirm that our own stellar models reproduce a well-defined period–companion mass relation irrespective of the details of the mass transfer process. With magnetic braking this relation extends to periods of less than 1 d for a $1 M_{\odot}$ giant donor. With this and the measured binary mass functions we calculate the orbital inclination of each system for a given pulsar mass. We expect these inclinations to be randomly oriented in space. If the masses of the pulsars were typically $1.35 M_{\odot}$ then there would appear to be a distinct dearth of high-inclination systems. However if the pulsar masses are more typically 1.55 to $1.65 M_{\odot}$ then the distribution of inclinations is indeed indistinguishable from random. If it were as much as $1.75 M_{\odot}$ then there would appear to be an excess of high-inclination systems. Thus with the available data we can argue that the neutron star masses in binary millisecond pulsars recycled by mass transfer from a red giant typically lie around $1.6 M_{\odot}$ and that there is no preferred inclination at which these systems are observed. Hence there is reason to believe that pulsar beams are either sufficiently broad or show no preferred direction relative to the pulsar’s spin axis which is aligned with the binary orbit. This is contrary to some previous claims, based on a subset of the data available today, that there might be a tendency for the pulsar beams to be perpendicular to their spin.

Key words: stars: neutron - stars: mass-loss - stars: evolution - pulsars: general - binaries: close

1 INTRODUCTION

Millisecond pulsars (MSPs) are radio pulsars with pulse periods canonically defined to be less than 30 ms. About 90 per cent of MSPs are found in binary systems (BMSPs). From their spin-down rates, these are estimated to have magnetic fields of between 10^7 and 10^9 G, significantly lower than the $10^{12} - 10^{13}$ G of ordinary radio pulsars (Lorimer 2008). In the standard rejuvenation model of BMSPs (Alpar et al. 1982; Radhakrishnan & Srinivasan 1982) the field decays and the pulsar spins up as matter is accreted from a companion star during a previous phase of evolution as a low- or intermediate-mass X-ray binary (LMXB/IMXB). The discovery of several X-ray pulsars with millisecond periods in

LMXBs and of IGR J18245–2452, an LMXB with a rotation period of 3.9 ms that alternates between a rotation-powered radio source and an accretion-powered X-ray source (Papitto et al. 2013) have provided strong evidence in support of a rejuvenation model. The precise nature of the evolution or decay of the magnetic field during accretion and the amount of mass accreted along the different binary pathways remains unresolved but must depend both on the origin of the field and the evolutionary history of BMSPs.

The lowest-mass neutron stars are expected to form by electron capture in the cores of the most massive asymptotic giant branch stars (Sugimoto & Nomoto 1980). An electron degenerate core collapses, as electrons are captured by ^{24}Mg and ^{20}Ne , at a mass of $1.375 M_{\odot}$ (Nomoto

1984). The cores of more massive stars collapse only after burning to iron-group elements and exceeding the Chandrasekhar limit. Some of this baryonic mass, depending on the equation of state of neutron stars, is lost to gravitational binding energy. Schwab, Podsiadlowski & Rappaport (2010) propose that neutron stars formed by electron capture are typically born with gravitational masses of around $1.25 M_{\odot}$ while those formed by iron core collapse with masses around $1.35 M_{\odot}$. Rejuvenation and spin up to millisecond periods requires accretion of at least $0.1 M_{\odot}$ or so of material from the inner edge of a Keplerian accretion disc. Zhang et al. (2011) find measured masses of the neutron stars in millisecond pulsars now to be around $1.55 M_{\odot}$. Here we are able to test whether the data for all BMSPs with helium white dwarf companions are consistent with such masses.

In an early study of the fastest BMSPs based on 30 stars it was noted that some 30 per cent showed the presence of a strong interpulse separated by 180° from the main pulse while this is the case for only a few per cent of the general sample of radio pulsars (Jayawardhana & Grindlay 1996). This was interpreted as evidence for nearly orthogonal rotators, in which the magnetic dipole axis is perpendicular to the spin axis. Subsequently Chen, Ruderman & Zhu (1998) argued for a bimodal distribution of both nearly orthogonal and nearly aligned rotators among the galactic BMSPs. Ruderman & Chen (1999) presented theoretical arguments in favour of these findings based on a specific superfluid and superconducting model for the evolution of field in spinning accreting neutron stars. Subsequently Backer (1998) analysed the minimum masses of a sample of low-mass BMSPs assuming that the orbital inclinations were randomly oriented in space but with further specific assumptions on the neutron star and white dwarf masses and presented evidence apparently lending support to the orthogonal rotator model.

The stellar properties of any companion along with its orbit point to the evolutionary pathway by which the BMSP reached its current state. Hurley et al. (2010) made comprehensive binary population syntheses and described the numerous routes to MSPs and the expected relation between the final companion mass and the orbital period after mass transfer. Notably they included the possibility that the neutron star began accreting as a massive ONe white dwarf that collapsed to the pulsar after accreting sufficient mass (accretion induced collapse). Here we focus on what appears to be a rather common route in which an evolved low- to intermediate-mass star fills its Roche lobe before core helium ignition but after core hydrogen exhaustion. This sequence is apparent in the figures of Hurley et al. (2010) whether or not the neutron star is formed by accretion induced collapse.

In this paper we have undertaken a detailed statistical study of the significantly enhanced current sample of millisecond pulsars with helium white dwarf companions with their well determined mass functions derived from quantities given in the Australia Telescope National Facility (ATNF) pulsar catalogue. Our study is similar to that of Stairs et al. (2005) but the increase in data mean we can now make somewhat more significant conclusions.

Our analysis indicates that good overall agreement with the totality of observations of BMSPs with He white dwarf companions can be achieved if the masses of the neutron lie typically around $1.6 M_{\odot}$ which is higher than what is expected from typical electron-capture or core-collapse super-

novae but is consistent with expectations of the re-cycling hypothesis. There is no significant difference in this consistency between low- and high-period systems as was suggested by Stairs et al. (2005). Nor can we agree with the conclusion of Backer (1998) in support of orthogonal rotators.

2 DETAILED MODELS OF RLOF

We compute an extensive grid of models with the Cambridge STARS code. In all cases we fully compute the evolution of the low-mass donor star while the neutron star is treated as a point mass accretor. The donors begin their evolution as a zero-age main-sequence stars in thermal equilibrium. With a series of models we investigate the effect of different binary parameters on the M_c - P_{orb} relation for the whole range of Case B RLOF. In the terminology of Kippenhahn & Weigert (1967) Case B refers to mass transfer that begins after the exhaustion of hydrogen fuel in a star's core but before ignition of helium. We refer to late Case B when mass transfer begins after the star is established on the giant branch, early Case B when it begins when the star is crossing the Hertzsprung gap and very early Case B when it begins at the tip of the main-sequence once the star has a helium core but before it begins its excursion to the red in the H-R diagram.

2.1 Cambridge STARS Code

We use a version of the Cambridge STARS code (Eggleton 1971; Pols et al. 1995) updated by Stancliffe & Eldridge (2009). The code features a non-Lagrangian mesh. Convection is according to the mixing-length theory of Böhm-Vitense (1958) with $\alpha_{\text{MLT}} = 2$ and convective overshooting is included as described by Schröder, Pols & Eggleton (1997). The nuclear species ^1H , ^3He , ^4He , ^{12}C , ^{14}N , ^{16}O and ^{20}Ne are evolved in detail. Opacities are from the OPAL collaboration (Iglesias & Rogers 1996) supplemented with molecular opacities of Alexander & Ferguson (1994) and Ferguson et al. (2005) at the lowest temperatures and by Buchler & Yueh (1976) at higher temperatures. Electron conduction is that of Hubbard & Lampe (1969) and Canuto (1970). Nuclear reaction rates are those of Caughlan & Fowler (1988) and the NACRE collaboration (Angulo et al. 1999).

2.2 Period – white dwarf mass relation

For the donor stars the luminosity depends only on the helium core mass and the radius depends only on the luminosity and the total mass Paczyński (1971) so there is a relation between the orbital period P_{orb} and the remnant mass M_c when the system detaches (Refsdal & Weigert 1971). We do not expect the M_c - P_{orb} relation to depend on how the system gets to this point so that details of how conservative is the mass transfer do not matter. Nor does the relation depend on the neutron star mass because for low enough mass ratios the Roche lobe radius is proportional to the ratio of the separation to the total mass of the system and by Kepler's third law the cube root of the square of the orbital period is proportional to this same ratio. Thus P_{orb} is

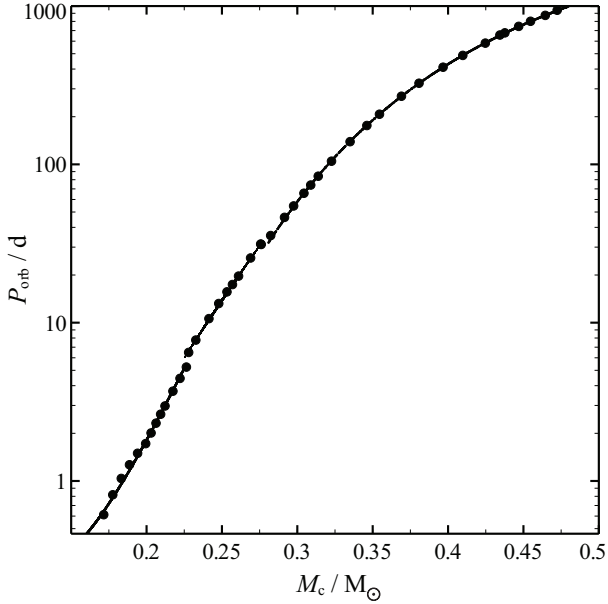


Figure 1. Our Canonical $P_{\text{orb}} - M_c$ relation. Points are a subset of our models made with $1 M_{\odot}$ donor stars in binary systems with neutron star companions of $1.55 M_{\odot}$ (circles). The solid line is our empirical fit (equation 2).

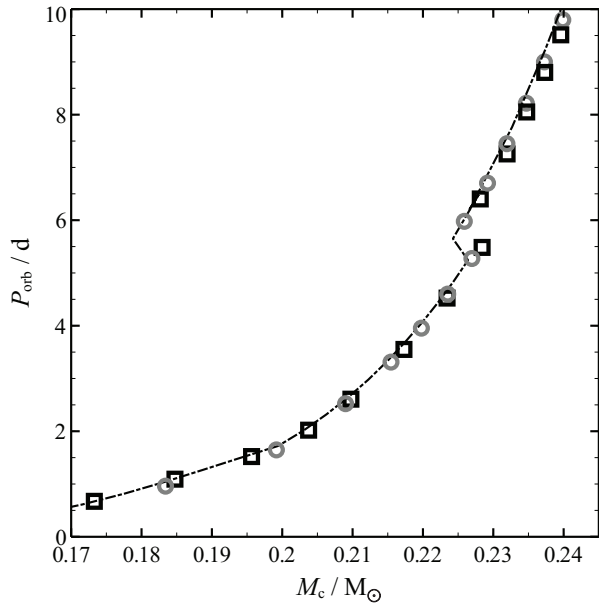


Figure 2. Variation of initial donor mass. Models made with a $0.875 M_{\odot}$ donor are open squares and models made with a $1.2 M_{\odot}$ donor are light open circles. The dot-dashed line is our canonical relation from $1 M_{\odot}$ donors.

a function only of M_c . We demonstrate that this is the case in the following sections.

Though the mass transfer to MSPs is likely to be non-conservative we first consider the canonical, perhaps extreme, fully conservative case in which all of the envelope of the donor star is transferred to and accreted by its companion and for which total angular momentum is conserved. We model initial donor masses of 0.875 , 1 and $1.2 M_{\odot}$. We give

the companion an initial mass of $1.55 M_{\odot}$. We demonstrate later that the relation is not affected by the non-conservative nature of the mass transfer. For each donor mass we evolve a set of 300 models with initial periods to cover the full range of Case B RLOF for each of the different donor masses. Magnetic braking, as discussed in more detail in the next section, is necessary to reach the lowest periods and core masses. Fig. 1 shows a subset of the $1 M_{\odot}$ donor models plotted with an empirical fit for the relation (section 2.5). In Fig. 2 we plot the $P_{\text{orb}} - M_c$ relation for a selection of models with each of the three initial donor masses. There is no perceptible difference. Lower-mass donor stars exhibit very similar behaviour to the $1 M_{\odot}$ donor once they evolve past the main sequence. However they are not expected to have evolved within the lifetime of the Galaxy. Higher mass donors, once established on the giant branch undergo unstable RLOF which probably leads to common-envelope evolution and perhaps merging of the stars. Thus in general we do not expect the donor star mass to lie outside the range $0.875 - 1.2 M_{\odot}$ very often and so we take the $P_{\text{orb}} - M_c$ relation derived from $1 M_{\odot}$ donors to be canonical. There are some discontinuities apparent for all donor masses around a remnant mass of $0.225 M_{\odot}$ caused by dredge up of the previously burnt stellar interior by the deepening convective envelope.

2.3 Short Periods and Magnetic Braking

The minimum white dwarf mass that can be left by a given donor depends on the Schönberg–Chandrasekhar mass (Schönberg & Chandrasekhar 1942) of its core. Beyond this the core cannot remain isothermal and still support the stellar envelope. After this the star evolves rapidly across the HG. If evolved fully conserving mass and angular momentum our $1 M_{\odot}$ donor leaves a minimum remnant mass of $0.22 M_{\odot}$.

A group of very short orbital period MSPs are thought to have evolved from LMXBs (Fabian et al. 1983) for which the mass transfer is driven by orbital angular momentum loss rather than stellar evolution. In these systems the, typically low initial mass ($M_d < 0.9 M_{\odot}$) donor star does not develop a degenerate core and final periods are a few hours.

With their shorter hydrogen-burning lifetime intermediate-mass donors, those around $1 M_{\odot}$ and more, can develop helium cores but are also expected to suffer magnetic braking if their orbital period is short enough. If such an evolved intermediate-mass star begins RLOF before this (very early Case B) its limiting core mass is reduced as it transfers mass and so consequently behaves as if it were a star with a somewhat lower initial total mass. There is a bifurcation period below which systems evolve as LMXBs to very low P_{orb} and above which they evolve to larger P_{orb} transferring mass as red giants or subgiants. We are interested in these latter systems which end up detached with $P_{\text{orb}} \gtrsim 1$ d.

We include magnetic braking at the empirical rate of Verbunt & Zwaan (1981),

$$\frac{\dot{J}}{J} = -0.5 \times 10^{-28} \text{ s}^2 \text{ cm}^{-2} f_{\text{mb}}^{-2} \frac{I R_d^2}{a^5} \frac{GM^2}{M_a M_d} \text{ s}^{-1}, \quad (1)$$

where R_d is the radius of the donor star, I its moment of inertia, a the semi-major axis of the orbit, M the total mass

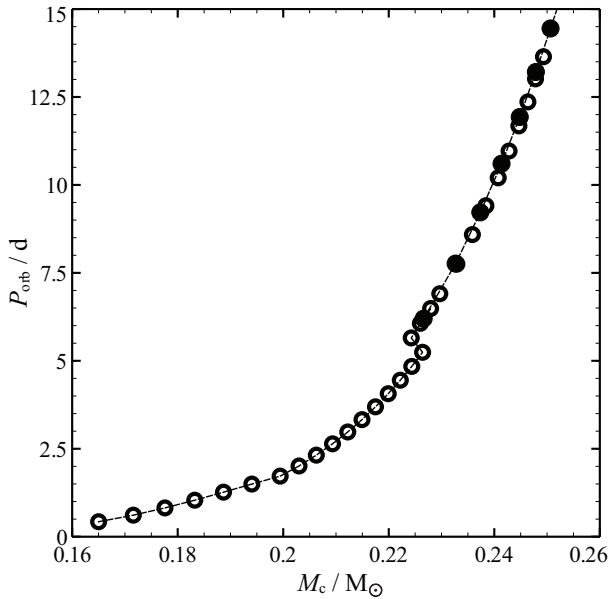


Figure 3. Detail of the period–core mass relation for critically braked systems (open circles) compared with non-braked systems (solid circles). All models have $1.55 M_{\odot}$ neutron star that accreted from an initially $1 M_{\odot}$ donor.

of the binary system, M_a the mass of the accretor and M_d is the mass of the donor. The factor f_{mb} was chosen to fit the equatorial velocities of G and K type stars (Smith 1979).

Fig. 3 shows detail of the low-period end of the $P_{orb} - M_c$ relation for systems evolved with and without magnetic braking. The form of the magnetic-braking law is such that the initial orbital periods for which it can produce lower-period systems with He white dwarfs is finely balanced between 2 and 2.2 d to produce final periods between 0.5 and 6 d.

2.4 Examples of evolution

Fig. 4 shows a Hertzsprung–Russell diagram for three binary star models (B, C and D) that begin RLOF at different stages along with a track (A) for single star evolution. Model B begins RLOF only once established as a red giant, late Case B. Model C is crossing the Hertzsprung gap, begins RLOF as a subgiant, early case B, while model D begins mass transfer with an isothermal gas-pressure supported core, very early Case B. By the time the stars in models C and D detach they have established degenerate He cores and are ascending the red giant branch. The larger the initial period, the further up the giant branch the RLOF begins. Mass transfer strips the envelope to reveal the stars’ cores which then cool to become white dwarfs.

2.5 Empirical fit

A good empirical fit to $P_{orb} - M_c$ relation for all the models with $1 M_{\odot}$ donors, including those with magnetic braking, is given by

$$P_{orb}/d = \exp(a + (b/(M_c/M_{\odot})) + c(\ln(M_c/M_{\odot}))), \quad (2)$$

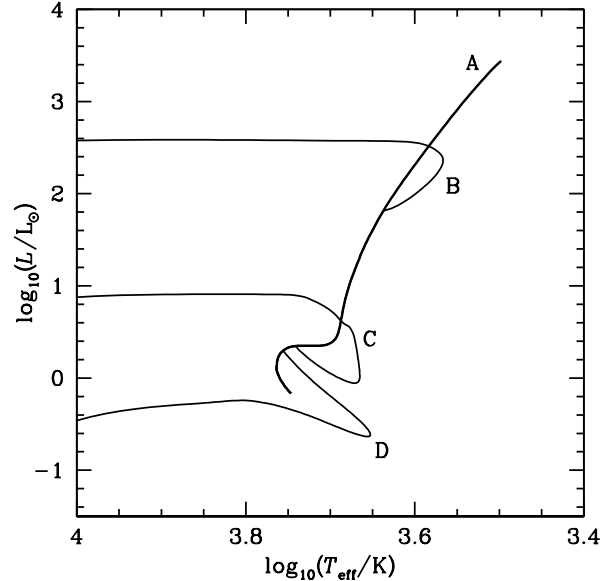


Figure 4. A Hertzsprung–Russell diagram, in the bolometric luminosity L –effective temperature T_{eff} plane, for the evolution of an isolated $1 M_{\odot}$ star (labelled A), along with the evolution of similar stars in binary systems with neutron star companions of $1.55 M_{\odot}$. All have active magnetic braking. Model B has an initial orbital period of 2 d, model C 2.14 d and D 20 d.

with

$$(a, b, c) = \begin{cases} (22.902, 3.097, 23.483) & \text{for } 0.17 \leq M_c < 0.225 \\ (14.443, 0.335, 9.481) & \text{for } 0.225 \leq M_c < 0.28 \\ (11.842, -3.831, -4.146) & \text{for } 0.28 \leq M_c < 0.48. \end{cases} \quad (3)$$

2.6 Measured pulsar masses

Table 1 lists observed MSP – white dwarf binary systems that have measured pulsar masses and companion masses. These masses are generally higher than those found for isolated pulsars (Zhang et al. 2011). This may be due to either a range in initial neutron star mass or accretion during the mass transfer. Tauris & Savonije (1999) noticed a negative correlation between the orbital period and the mass of the pulsar. In Fig. 5 we plot the data for the systems in Table 1. Any correlation is actually rather weak. Though we list all the measured masses here we note that all of those with orbital periods of less than 1 d are excluded from our analysis because they may have undergone Case A mass transfer, while the star is still burning hydrogen in its core, rather than Case B mass transfer. Indeed B1957+20 is a black widow pulsar (Fruchter et al. 1988) with a low-mass main-sequence star, rather than a white dwarf. J1910–5959A is also excluded because it is a member of a globular cluster (Corongiu et al. 2012). J2016+1948 is excluded because it has $P_{spin} > 30$ ms and J1614–2230 is excluded because it has a companion mass larger than $0.472 M_{\odot}$.

De Vito & Benvenuto (2010) looked at the effect of the neutron star mass on these systems and found that, for systems of given initial orbital period and initial donor star mass, the mass of the neutron star heavily affects the evo-

Table 1. BMSPs with measured pulsar and companion masses. Two systems with $P_{\text{spin}} > 30$ ms are included for completeness but are excluded from our analysis.

Name	$P_{\text{spin}}/\text{ms}$	P_{orb}/d	M_{p}/M_{\odot}	$M_{\text{comp}}/M_{\odot}$	Reference
J0348+0432	39.12	0.103	2.01 ± 0.04	0.172 ± 0.003	Antoniadis et al. (2013)
J0751+1807	3.48	0.26	1.26 ± 0.14	0.191 ± 0.015	Nice, Stairs, & Kasian (2008)
J1738+0333	5.85	0.35	1.47 ± 0.06	0.181 ± 0.006	Antoniadis et al. (2012)
B1957+20	1.61	0.38	2.40 ± 0.12	0.035 ± 0.002	Gonzalez et al. (2011)
J1012+5307	5.26	0.60	1.6 ± 0.2	0.16 ± 0.02	van Kerkwijk et al. (2005)
J1910-5959A	3.27	0.84	1.33 ± 0.11	0.180 ± 0.018	Corongiu et al. (2012)
J1909-3744	2.95	1.53	1.438 ± 0.024	0.2038 ± 0.0022	Jacoby et al. (2005)
J0437-4715	5.76	5.74	1.76 ± 0.02	0.254 ± 0.014	Verbiest et al. (2008)
J1614-2230	3.15	8.69	1.97 ± 0.04	0.500 ± 0.006	Demorest et al. (2010)
B1855+09	5.36	12.33	1.6 ± 0.2	0.270 ± 0.025	Splaver (2004)
J1910+1256	4.99	58.47	1.6 ± 0.6	$0.30 - 0.33$	Gonzalez et al. (2011)
J1713+0747	7.99	67.83	1.3 ± 0.2	0.28 ± 0.03	Splaver et al. (2005)
J1853+1303	4.09	115.65	1.4 ± 0.7	$0.33 - 0.37$	Gonzalez et al. (2011)
J2016+1948	64.95	635.04	1.0 ± 0.5	$0.43 - 0.47$	Gonzalez et al. (2011)

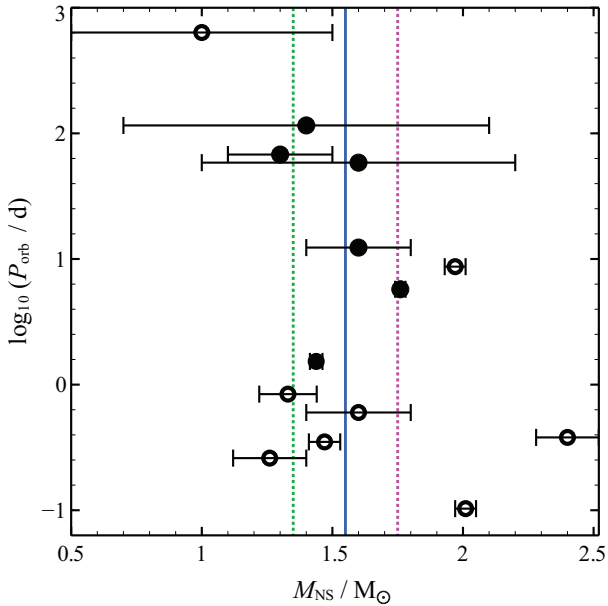


Figure 5. Neutron star masses and orbital periods of the observed BMSPs listed in Table 1. Solid circles are the systems that fit our selection criteria while open circles are those that are excluded for various reasons. Vertical lines indicate masses of 1.35, 1.55 and 1.75 M_{\odot} .

lution. However they conclude that the M_c - P_{orb} relation is insensitive to the initial neutron star mass, confirming the prediction made by Rappaport et al. (1995). We tested the effect of the neutron star mass on the evolution of our binary systems by computing models that initially had a $1 M_{\odot}$ donor star and neutron star masses of 1.35, 1.55 and 1.75 M_{\odot} . We made 100 models for each case with initial orbital periods spanning the entire M_c - P_{orb} relation. Fig. 6 shows the M_c - P_{orb} relations for a subset of these models with initial periods between 2 to 2.4 d. The M_c - P_{orb} relation itself is not affected by the neutron star mass but, for a given initial orbital period, the higher the neutron star mass, the more massive the predicted white dwarf remnant.

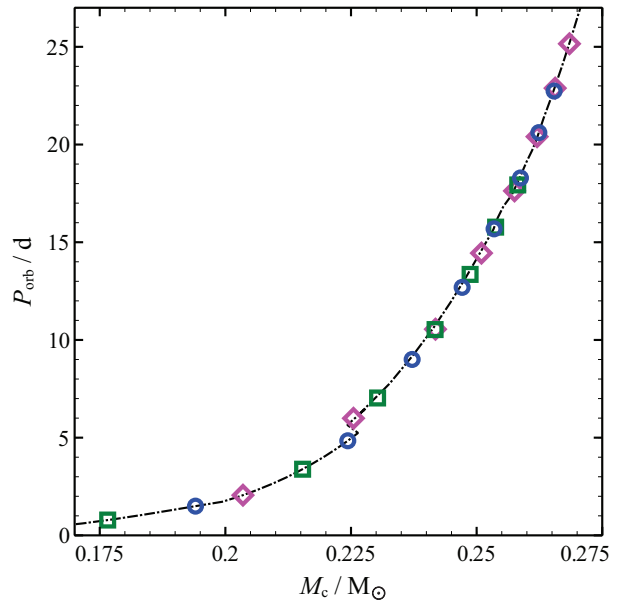


Figure 6. The effect of neutron star mass on the M_c - P_{orb} relation. Three cases are shown here, all models have a $1 M_{\odot}$ donor star and were computed with initial periods from 2 d to 2.4 d. Open squares have an initial neutron star mass of 1.35 M_{\odot} , open circles 1.55 M_{\odot} and open diamonds 1.75 M_{\odot} . The dot-dashed line is our empirical fit. As expected the neutron star mass has no effect on the $P_{\text{orb}} - M_c$ relation.

The higher mass of neutron star lies further up the relation but not off it.

However the neutron star mass does matter when we compute orbital inclinations (equation 11). For now we conclude that masses of MSPs in systems that could have helium white dwarf companions lie between about 1.35 and 1.75 M_{\odot} and cluster around 1.55 M_{\odot} .

2.7 RLOF Efficiency

Relaxing conservative evolution further, we allow mass to be lost from either star during mass transfer. The total angular

momentum J is the sum of the orbital angular momentum and the rotational (or spin) angular momentum of each star. The latter is typically only 1–2 per cent of the orbital angular momentum and so can usually be ignored though we do include it in our detailed stellar models. Tauris & Savonije (1999) argued that the accretion process is inefficient, with only a small portion of transferred matter accreted by the neutron star. The rest is ejected. Burderi et al. (2005) confirmed that the accretion process in these systems is non-conservative. Only $0.1 M_{\odot}$ of material from the inner edge of the disc is needed to spin up the neutron star to periods below one millisecond. De Vito & Benvenuto (2012) computed the evolution of a set of models with initial donor star between 0.5 and $3.5 M_{\odot}$, initial orbital periods between 0.175 and 12 d and initial neutron stars masses between 0.8 and $1.4 M_{\odot}$, with varying degrees of mass transfer efficiency. Following their approach we define efficiency parameters α , the fraction of mass lost by the donor that is transferred to the accretor and β , the amount of matter actually captured by the accretor. A fraction $1 - \alpha$ of the mass lost by the donor then carries off the specific angular momentum of the donor while a fraction $\alpha(1 - \beta)$ of the mass lost by the donor carries off the specific angular momentum of the accretor. So

$$\dot{M}_a = -\alpha\beta\dot{M}_d, \quad (4)$$

and

$$\dot{J} = (1 - \alpha)\dot{M}_d a_2^2 \omega + \alpha(1 - \beta)\dot{M}_d a_1^2 \omega. \quad (5)$$

Thence

$$\frac{\dot{J}}{J} = \frac{(1 - \alpha)\dot{M}_d a_2^2 \omega + \alpha(1 - \beta)\dot{M}_d a_1^2 \omega}{(M_a M_d / (M_a + M_d)) a^2 \omega}, \quad (6)$$

where $J = M_a M_b a^2 \omega / (M_a + M_b)$ is the orbital angular momentum for semi-major axis a and orbital angular velocity $\omega = 2\pi / P_{\text{orb}}$. This simplifies to

$$\frac{\dot{J}}{J} = \frac{\dot{M}_d}{M_d} \left[\frac{1 - \alpha + \alpha(1 - \beta)q^2}{1 - q} \right]. \quad (7)$$

where the mass ratio $q = M_d / M_a$.

We evolved sets of 100 models for combinations of α and β , with initial orbital periods in the range 2 to 3 d. Fig. 7 illustrates the effects on the $M_c - P_{\text{orb}}$ relation. As expected the relation between M_c and P_{orb} is not much affected by the non-conservative nature of the RLOF but, for a given initial orbital period, increasing α or decreasing β leaves a more massive core and consequently a longer final period because, even though the escaping material carries away angular momentum, the total system mass falls.

2.8 Comparison of Detailed Models and Data

The systems with measured neutron star masses listed in Table 1 also have measured companion masses. We again ignore systems with $P_{\text{orb}} < 1$ d. Note that J1614–2230 is also excluded because to fit the data and the $P_{\text{orb}} - M_c$ relation would require too small a neutron star mass (see Section 4). This is encouraging because it is indeed found to have a companion of $0.5 M_{\odot}$, too massive for a He white dwarf. We plot the remaining data in Fig. 8 and find that the fit with our canonical relation is good given the measurement errors.

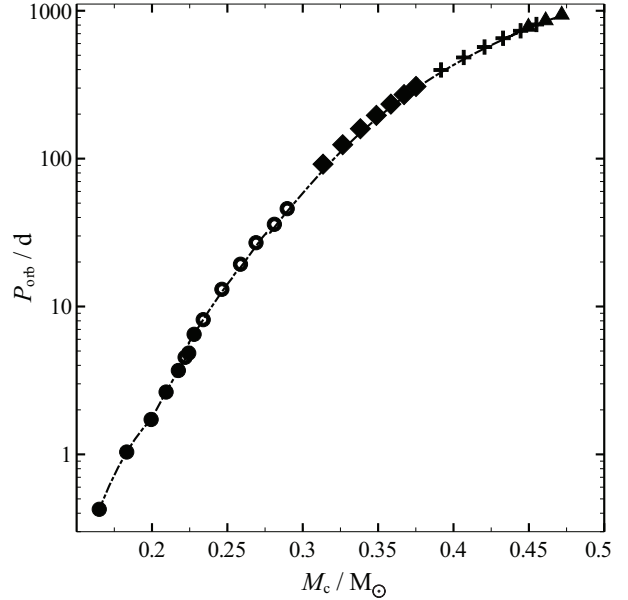


Figure 7. The effect of varying the RLOF efficiency on the $M_c - P_{\text{orb}}$ relation. Five cases are shown, 1) $\alpha = \beta = 1$ (solid circles), 2) $\alpha = \beta = 0$ (open circles), 3) $\alpha = 1$ and $\beta = 0.6$ (diamonds), 4) $\alpha = 0.6$ and $\beta = 0$ (crosses) and 5) $\alpha = 1$ and $\beta = 0$ (triangles). Each set initially has $M_d = 1 M_{\odot}$, $M_a = 1.55 M_{\odot}$, and $2 < P_{\text{orb}}/d < 2.19$. The dot-dashed line is our canonical relation.

Note that J2016+1948 is also formally excluded because its spin period exceeds 30 ms but we plot it here because it lies on the canonical $P_{\text{orb}} - M_c$ relation. This suggests that it has passed through a similar evolution but has just not been spun up so much.

2.9 Donor Star Metallicity

We are concentrating on BMSPs in the Galactic field and so do not expect the metallicity to vary much from solar. However we investigated how the metallicity of the donor star affects our $M_c - P_{\text{orb}}$ relation by evolving two further sets of models with $Z = 0.01$, half solar, and $Z = 0.03$, one and a half solar. As metallicity falls opacity drops and stars are smaller for the same luminosity and hence core mass so the final orbital period for a given white dwarf mass is smaller. The results are shown in Fig. 9. The change in the relation with metallicity is larger than for any of the other effects we have tested but all three models remain in good agreement with the observed systems.

2.10 Comparison with Previous Work

The relation between the mass of the white dwarf remnant and the orbital period after mass transfer ($M_c - P_{\text{orb}}$) has been computed a number of times in the past. Rappaport et al. (1995) used 11 stellar models with various masses between 0.8 and $2 M_{\odot}$, computed by Han, Podsiadlowski & Eggleton (1994) with Eggleton’s STARS code (Eggleton 1971) to obtain the relation between the radius of a star on the red giant branch and its core mass in the range 0.15 to $1.15 M_{\odot}$. They then used this to derive a $M_c - P_{\text{orb}}$ relation. Tauris & Savonije (1999)

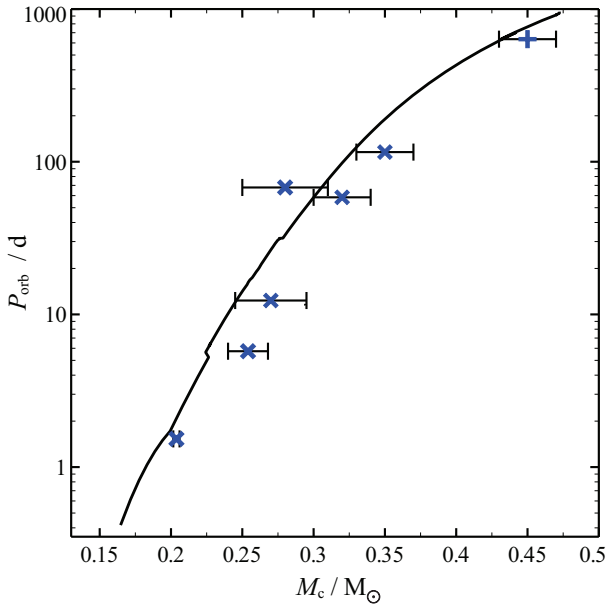


Figure 8. MSPs with measured companion masses in the M_c – P_{orb} plane. The solid line is our canonical relation. We do not include systems excluded from our analysis except for the 635 d system J2016–2230 (shown by +). It appears to lie precisely on the relation but has a spin period of 65 ms.

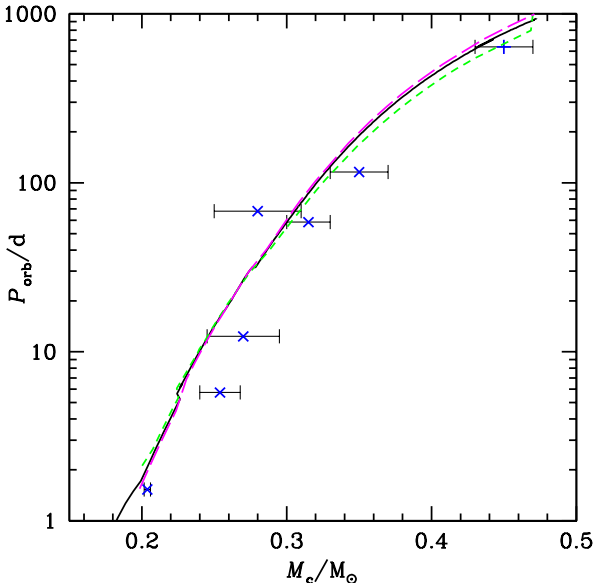


Figure 9. The effect of donor star metallicity on the M_c – P_{orb} relation. Models are all for accretion on to a $1.55 M_{\odot}$ neutron star from a $1 M_{\odot}$ donor. The solid line has $Z = 0.02$, the short-dashed line $Z = 0.01$ and the long-dashed line $Z = 0.03$. The effect of changing metallicity over the range that might be expected in the Galactic field is still rather small but larger than any effect owing to the nature of the mass transfer.

conducted a detailed study of the thermal response of the donor star to mass loss in order to examine the evolution of the mass transfer (non-conservative in this case) and to monitor its stability. They used Eggleton’s STARS code to compute 121 models of the evolution of different binary systems, with a low-mass donor and a neutron star companion, through stable mass transfer. Their donor masses between 1 and $2 M_{\odot}$, a neutron star of $1.3 M_{\odot}$ and initial orbital periods between 2 and 800 d. They obtained M_c – P_{orb} relations and devised fitting formulae for various chemical compositions. Podsiadlowski, Rappaport & Pfahl (2002) made a systematic study of low- and intermediate-mass binary systems with donor masses from 0.6 to $7 M_{\odot}$ (a much wider range than Tauris & Savonije 1999) a neutron star of $1.4 M_{\odot}$ and initial orbital periods between 0.17 and 100 d. They used an updated version of the stellar evolution code described by Kippenhahn, Weigert & Hofmeister (1967) to make 100 binary star models, in which half of the mass lost by the donor was accreted by the companion. Their models showed an enormous variety of evolutionary channels which they suggest may be the reason behind the diversity in the observed population of these systems. De Vito & Benvenuto (2010) made many detailed evolutionary models with a wide range of donor (0.5 to $3.5 M_{\odot}$) and accretor (0.8 to $1.4 M_{\odot}$) masses and orbital periods at the onset of Roche lobe overflow from 0.5 to 12 d with a code described by Benvenuto & De Vito (2003). Their models show signs of departure from the Rappaport M_c – P_{orb} relation at core masses below $0.25 M_{\odot}$ but are in better agreement with the M_c – P_{orb} relation found by Tauris & Savonije (1999). They studied the dependence of the neutron star mass on the M_c – P_{orb} relation and later the dependence of the mass transfer efficiency on the M_c – P_{orb} relation (De Vito & Benvenuto 2012). Shao & Li (2012) explored low- and intermediate-mass systems, similarly to Podsiadlowski et al. (2002), with the Cambridge STARS code, with donor masses of 1 to $6 M_{\odot}$ and accretor masses of 1.0 to $1.8 M_{\odot}$. They modelled the M_c – P_{orb} relation for donors from 1 to $5 M_{\odot}$, compared their relations to observed possible MSP–helium white binaries and explored magnetic braking in these systems.

The fits of Tauris & Savonije (1999) have been most extensively used in the past so we compare our models with theirs in Fig. 10. Their fits are of the form

$$\frac{M_{\text{wd}}}{M_{\odot}} = \left(\frac{P_{\text{orb}}}{b} \right)^{1/a} + c, \quad (8)$$

with

$$(a, b, c) = \begin{cases} (4.50, & 1.2 \times 10^5, & 0.120) & \text{Pop.I,} \\ (5.00, & 1.0 \times 10^5, & 0.100) & \text{Pop.II,} \end{cases} \quad (9)$$

for population I stars and population II stars. Our models compare well with their population I stars. Despite the fact that lower metallicities are a better fit to two of the measured companion masses we use solar metallicity because we exclude BMSPs in globular clusters. The remaining systems fit better or equally well at solar metallicity.

3 SELECTION OF BMSPS

The ATNF catalogue (Manchester et al. 2005) currently lists 293 BMSPs with $P_{\text{spin}} \leq 30$ ms. Of these 101 are in the

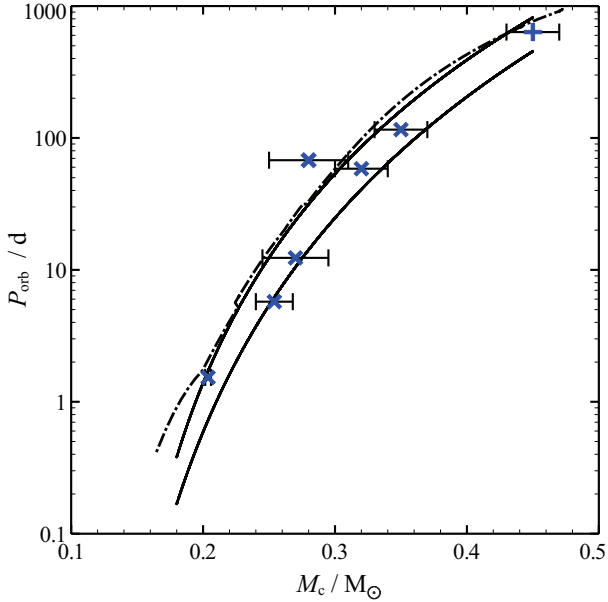


Figure 10. Comparison with the work of Tauris & Savonije (1999). The dot-dashed line is our canonical relation. The two solid curves are fits of Tauris & Savonije (1999) for population I stars (leftmost) and population II stars (rightmost).

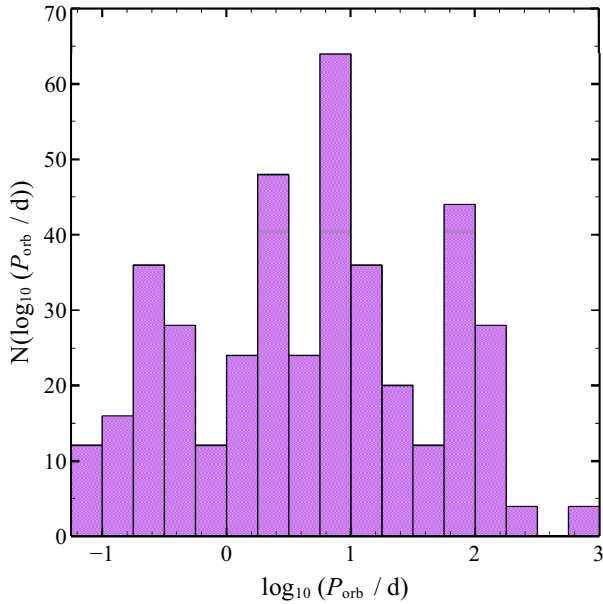


Figure 11. The distribution of all BMSPP orbital periods less than 1,000 d. Those systems with $P_{\text{orb}} > 940$ d are not expected to have helium white dwarf companions. Below the gap apparent around $P_{\text{orb}} = 1$ d we can expect contamination from systems that have undergone Case A mass transfer and now have low-mass hydrogen-rich companions.

Galactic field and have measured binary mass functions. It is important to exclude all BMSPPs that have not been recycled by accretion from a red giant with a helium core but otherwise we wish to test the hypothesis that all remaining systems did indeed form by this route. We exclude any BMSPPs in globular clusters because their formation can be more convoluted (Lorimer 2008). B1257+12 can be excluded di-

rectly because the orbit is for its planet of mass only $0.02 M_{\oplus}$ (Konacki & Wolszczan 2003) and J1502–6752 is excluded because it has an ultra-light companion (Manchester et al. 2005). Nor did we include B1620–26 because it is identified as being a multiple system in the ATNF pulsar catalogue so the other components in the system could have altered its evolution and J1903+0327 because it has a main-sequence star companion and is in a multiple system. Stars below $2.3 M_{\odot}$ suffer a helium flash when their degenerate core reaches $0.472 M_{\odot}$. This is the maximum mass that can be reached by a helium white dwarf companion and corresponds to a final orbital period of 940 d. Stars shrink during core helium burning and by the time they have grown sufficiently to fill their Roche lobes again their cores are generally above $0.5 M_{\odot}$. There is therefore a distinction between MSPs recycled by red giants with helium cores ($P_{\text{orb}} < 940$ d) and those recycled by asymptotic giants ($P_{\text{orb}} > 940$ d). This distinction is apparent in the figures of Hurley et al. (2010). We therefore impose an upper period limit of 940 d. At low orbital periods we must exclude systems in which mass transfer began while the donor star was still on the main sequence (Case A). The observed orbital period distribution for BMSPPs appears to have a gap between 0.73 d and 1.19 d (Fig. 11). Above this we can easily form systems with helium white dwarf companions when magnetic braking is included in our models. Below it there is likely to be contamination by systems that have undergone Case A mass transfer and still have a hydrogen-rich companion. We assume that the gap represents a good discriminator between the two populations and so exclude all systems with $P_{\text{orb}} < 1$ d. All the remaining systems are listed in Table A1 which can be found in the appendix. In practice we might expect most of the MSPs to have formed from relatively low-mass progenitors in electron-capture supernovae. In such stars degenerate cores collapse at $1.375 M_{\odot}$ (Nomoto 1984). They may lose about $0.1 M_{\odot}$ of their gravitational mass depending on the equation of state of the neutron star but then probably need to accrete a further $0.1 M_{\odot}$ to be spun up to millisecond periods. The measured masses listed in Table 1 suggest that the MSPs usually accrete more than this. Nevertheless, in the next section we describe how we further exclude systems that cannot fit the model with a neutron star less massive than $1.2 M_{\odot}$ and we use this rather conservative minimum to avoid excluding systems with the lowest measured masses of pulsars (Zhang et al. 2011). Only three systems need have a pulsar mass $1.2 < M_a / M_{\odot} < 1.35$.

4 ORBITAL INCLINATIONS

In the recycling model the MSP has been spun up by accretion through a disc of material transferred from a binary companion tidally locked to the binary orbit. The spin of the pulsar should then be aligned with the orbit. We expect orbital inclinations i to the line of sight to be uniformly distributed over a sphere so that the distribution of $\cos i$ should be flat.

Backer (1998) explored the spin periods, ages and magnetic fields of Galactic helium white dwarf MSPs. Modelling fixed masses for both the neutron star and the white dwarf, he concluded that observed inclinations are not randomly distributed but rather tend to be high. To explain this he

suggested that pulsar beams preferentially lie parallel to the orbital plane and so perpendicular to the pulsar spin axis. The following year Thorsett & Chakrabarty (1999) used the $M_c - P_{\text{orb}}$ relation derived by Rappaport et al. (1995) to conclude that the observed inclinations of binary MSPs are consistent with a random distribution. Stairs et al. (2005) similarly investigated a larger data set with the $M_c - P_{\text{orb}}$ relations of both Tauris & Savonije (1999) and Rappaport et al. (1995). They concluded that the existing forms of the $M_c - P_{\text{orb}}$ relations overestimate the white dwarf masses at large periods and are also in conflict for the shorter period system. With a Kolmogorov–Smirnov (KS) test on the cumulative distribution of orbital inclinations they found that the $M_c - P_{\text{orb}}$ relation of Tauris & Savonije (1999) is incompatible at the 99.5% level when they drew the pulsar masses from a Gaussian centred on $1.35 M_{\odot}$ with width $0.04 M_{\odot}$ (mirroring the neutron star mass distribution found by Thorsett & Chakrabarty 1999). Repeating the same investigation for neutron stars picked from a Gaussian centred on $1.75 M_{\odot}$ with width $0.04 M_{\odot}$ they reached agreement at the 50% level. Our analysis here is equivalent to that of Stairs et al. (2005) applied to a larger data set.

If the standard recycling model is correct we expect the systems to be oriented randomly in space so that the probability $P(i) di$ of finding an inclination i between i and $i + di$ should be such that $P(i) \propto \sin i$. We are interested exclusively in the systems that have periods within range of the $M_c - P_{\text{orb}}$ relations consistent with Case B RLOF. In the ATNF catalogue the minimum possible mass M_m , given the observed mass function and a pulsar mass of $1.35 M_{\odot}$ is listed. This can be transformed back to the binary mass function f by

$$f = \frac{(M_d \sin i)^3}{(M_a + M_d)^2} = \frac{M_m^3}{(1.35 M_{\odot} + M_m)^2}, \quad (10)$$

where M_a is the actual mass of the pulsar. We list the mass functions f in Table A1, along with the companion masses M_d obtained from P_{orb} with our canonical relation by a spline interpolation. For the combination of f and M_d there is a maximum mass M_{amax} of pulsar that can be accommodated in the system. We list in Table A1 too. When $M_{\text{amax}} < 1.2 M_{\odot}$ we exclude the system from the analysis. Such cases are marked with bullets. Note that all systems found to have an ATNF minimum companion mass $M_d > 0.5 M_{\odot}$, too large to be a He white dwarf and marked with stars in Table A1, are automatically excluded by this cut. Inclinations are then given by

$$i = \sin^{-1} \left(\frac{(f(M_a + M_d)^2)^{1/3}}{M_d} \right). \quad (11)$$

and we expect $\cos i$ to be uniformly distributed between 0 and 1 if the inclinations are consistent with being picked from a uniform distribution.

For each neutron star mass $M_a \in \{1.35, 1.55, 1.75\} M_{\odot}$ we calculate the inclinations for all remaining systems in Table A1. When the maximum permitted pulsar mass is less than the chosen M_a we assign $i = 90^\circ$ and thereby use $M_a = M_{\text{amax}}$ for such systems. Figs 12, 13 and 14 are histograms of the numbers of BMSPs over $\cos i$ split into two orbital period ranges for the three different choices of neutron star mass. There are 28 systems with $P_{\text{orb}} < 12$ d and 29 systems with longer periods. The distributions are reasonably uniform but

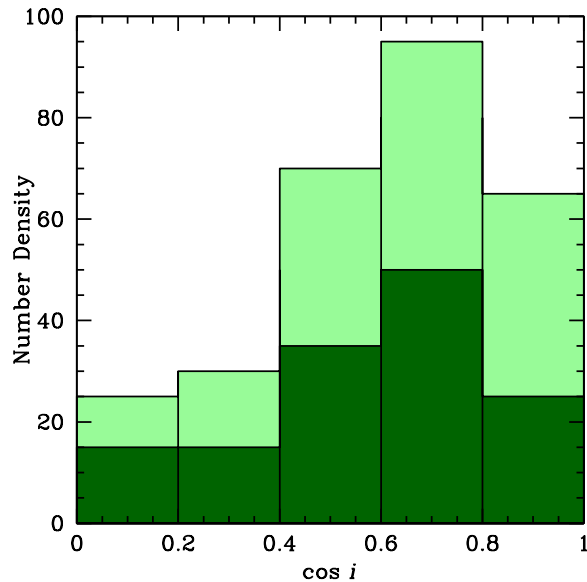


Figure 12. Histogram of the number density of the millisecond pulsar binary systems with respect to $\cos i$, assuming a current neutron star of mass $1.35 M_{\odot}$. The solid histogram is just the low-period systems (1 to 12 d), the lightly shaded histogram adds all the remaining high-period systems.

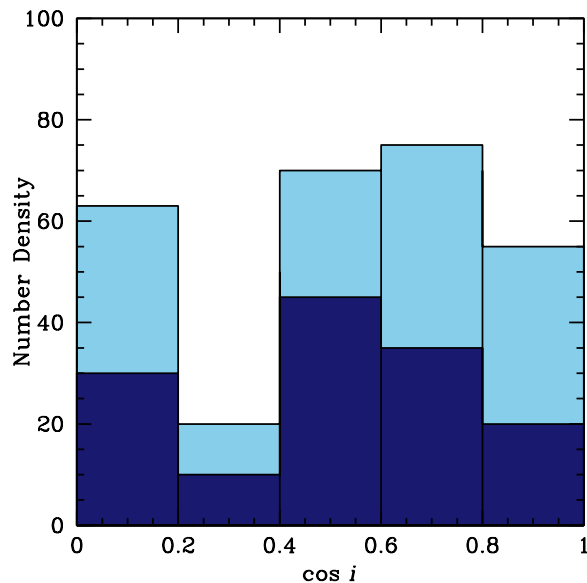


Figure 13. Histogram of the number density of the millisecond pulsar binary systems with respect to $\cos i$, assuming a current neutron star of mass $1.55 M_{\odot}$. The solid histogram is just the low-period systems (1 to 12 d) and the lightly shaded histogram adds all the remaining high-period systems.

show a distinct dearth of high inclination systems for $M_a = 1.35 M_{\odot}$. This is less extreme as M_a is raised to $1.55 M_{\odot}$ and becomes an excess when $M_a = 1.75 M_{\odot}$. To examine the significance of these trends we use Kolmogorov–Smirnov tests on the cumulative distributions of $\cos i$.

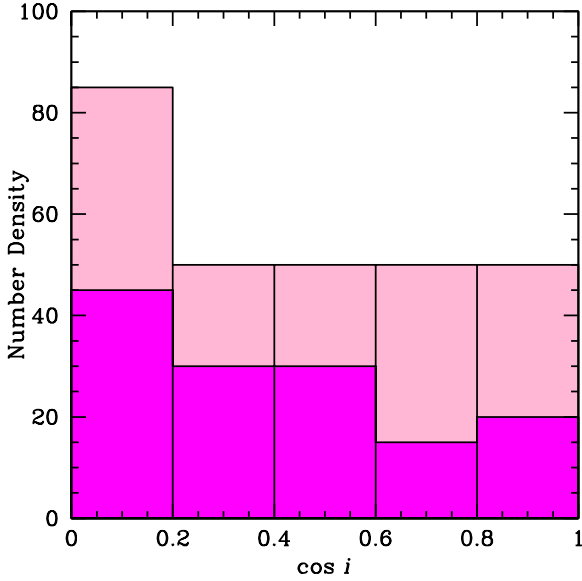


Figure 14. Histogram of the number density of the millisecond pulsar binary systems with respect to $\cos i$, assuming a current neutron star of mass $1.75M_{\odot}$. The solid histogram is just the low-period systems (1 to 12 d) and the lightly shaded histogram adds all the remaining high-period systems.

4.1 Kolmogorov–Smirnov tests

A KS test compares an observed cumulative distribution with a model. In this case we compare the observed distribution of $\cos i$ with a uniform distribution. The KS statistic D is the maximum difference between the observed cumulative distribution and the uniform cumulative distribution for any $\cos i$ and with this is associated the probability that D of this size or larger would be found for a sample of observations chosen at random from the uniform distribution (Press et al. 1992). Fig. 15 shows the cumulative distributions of $\cos i$ for the three pulsar masses compared with the uniform distribution. Recall that all the systems for which $M_a > M_{a,\max}$ have been assigned $\cos i = 0$ and this raises the $\cos i = 0$ end of each distribution in a perhaps biased manner. The results for $M_a = 1.35 M_{\odot}$ are however unaffected because the largest difference D is at larger $\cos i$. For the other two cases we take D to be the largest difference beyond the first data point that has $\cos i > 0$. This eliminates the bias by treating the highest inclination systems as if they were as uniformly distributed as possible.

Tables 2, 3 and 4 list the D and its significance for the three cases for all systems combined and split into orbital period ranges. We discard the system in the middle with $P_{\text{orb}} = 12.33$ d so that the two ranges have precisely the same number of systems and it is meaningful to compare the KS probabilities. For $M_a = 1.35 M_{\odot}$ there is a significant lack of high inclination systems and for $M_a = 1.75 M_{\odot}$ there is a significant excess and both of these can be ruled out given their very low KS probabilities. For $M_a = 1.55 M_{\odot}$ a distribution as different as observed would be found 35 times in 100 random samples so that the inclinations are consistent with a uniform distribution of orientations in space. Equivalent analysis for $M_a = 1.45 M_{\odot}$ gives a KS probability of 0.040 while for $M_a = 1.65 M_{\odot}$ it is 0.173. Neither of

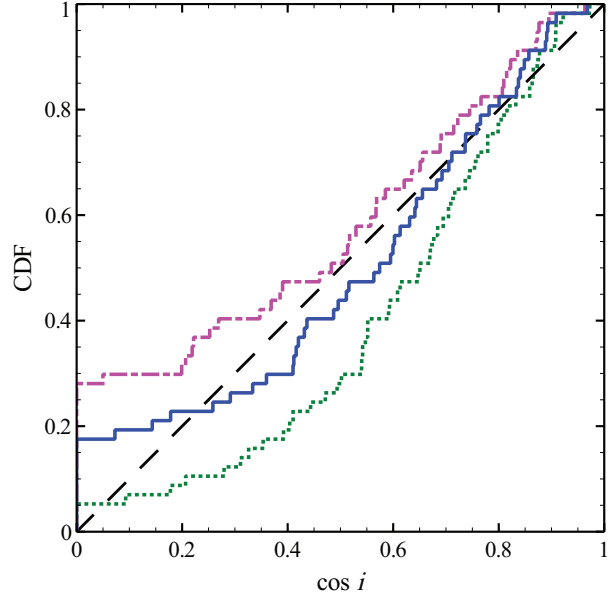


Figure 15. Cumulative distributions of $\cos i$. The expected uniform distribution is the dashed line. The blue solid line is for the data when we assume the pulsar masses are $1.55 M_{\odot}$ whenever possible and as large as possible otherwise. The dotted line is for $1.35 M_{\odot}$ pulsars and the dot-dashed line for $1.75 M_{\odot}$ pulsars. The up turn at $\cos i = 0$ is artificial because any system that cannot accommodate a neutron star of the appropriate mass is placed there. This artificial difference is not used for our KS tests.

Table 2. KS test on $\cos i$ for $M_a = 1.35 M_{\odot}$

M_a/M_{\odot}	P_{orb}/d range	D	Probability	N_{sys}
1.35	full	0.242	0.000201	57
1.35	< 12.3	0.257	0.0406	28
1.35	> 12.4	0.266	0.0307	28

these are small enough to really rule out such neutron star masses but we conclude that anything in the range around $1.55 \leq M_a/M_{\odot} \leq 1.65$ is quite acceptable. The KS test is weak for small data sets but this conclusion remains apparent for the low and high systems taken independently. When $M_a = 1.55 M_{\odot}$ the high probabilities of around one and two thirds mean there is no reason to suggest that the distribution or orbital inclinations changes with period in this case. However when $M_a = 1.75 M_{\odot}$ the fit for the low-period group is somewhat better than for the high-period group. This is consistent with what Stairs et al. (2005) found. However the numbers are still too small for this to be a significant conclusion, while the full distribution, likely to occur at random only once in about 2,000 samples, does significantly rule out such a large neutron star mass.

For comparison we apply the same analysis to the sample of MSPs used by Backer (1998) and with $M_a = 1.4 M_{\odot}$, as he assumed. Fig. 16 shows the cumulative distributions of $\cos i$ modelled with our canonical $P_{\text{orb}} - M_c$ and a neutron star mass of $1.4 M_{\odot}$, as chosen by Backer (1998). We exclude systems according to the same criteria we have used for the full sample and assign inclinations of $i = 90^\circ$ to

Table 3. KS test on $\cos i$ for $M_a = 1.55 M_\odot$

M_a/M_\odot	P_{orb}/d range	D	Probability	N_{sys}
1.55	full	0.120	0.359	57
1.55	< 12.3	0.181	0.286	28
1.55	> 12.4	0.142	0.591	28

Table 4. KS test on $\cos i$ for $M_a = 1.75 M_\odot$

M_a/M_\odot	P_{orb}/d range	D	Probability	N_{sys}
1.75	full	0.266	0.000470	57
1.75	< 12.3	0.122	0.772	28
1.75	> 12.4	0.236	0.0747	28

systems with $M_{a,\text{max}} < 1.4 M_\odot$. The KS probability of obtaining $D = 0.334$ or larger is 3.44×10^{-2} so that the data used by Backer (1998) actually show dearth of high inclinations just as we find with $M_a = 1.35 M_\odot$. Backer (1998) based his conclusion on a comparison between the distribution of minimum masses and a uniform distribution of $\sin i$. However it is the ratio of that minimum mass to the actual mass of the companion that is $\sin i$. In Fig. 17 we show the distribution of this ratio when we assume that the actual companion mass is known from P_{orb} . This distribution then shows a dearth of systems at large $\sin i$ quite contrary to his original claim. The conclusion that pulsar beams tend to be perpendicular to their spin axis is therefore no longer tenable.

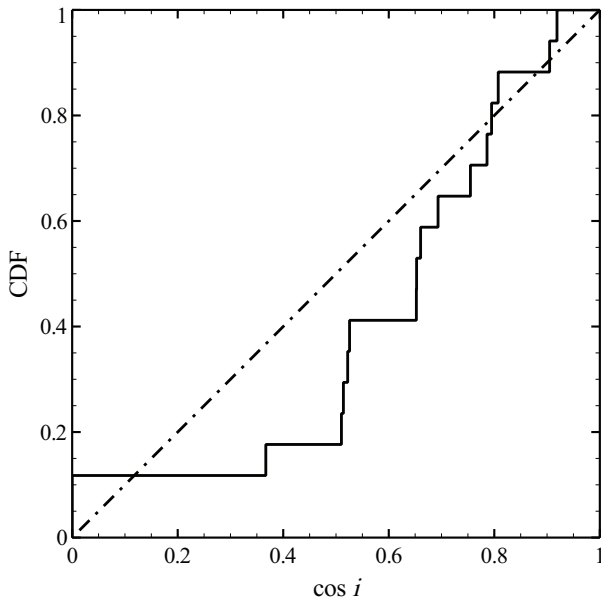


Figure 16. Cumulative distribution of $\cos i$ for the sample of 15 MSPs used by Backer (1998) that fit our selection criteria. The dot-dashed line is the CDF of the expected uniform distribution. The solid line is for Backer’s sample of systems with $P_{\text{orb}} > 1$ d obtained with our canonical $P_{\text{orb}} - M_c$ relation and a neutron star mass of $1.4 M_\odot$.

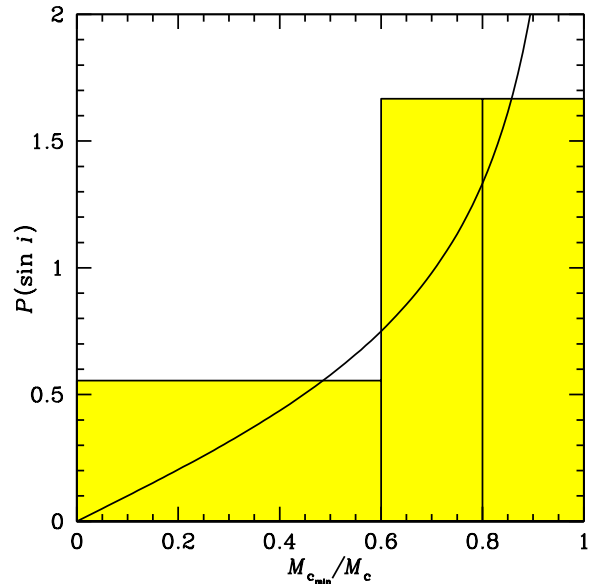


Figure 17. Histogram of the ratio of the minimum companion mass to a pulsar of $1.4 M_\odot$ to its actual mass if it lies on our $P_{\text{orb}} - M_c$ relation compared to the distribution of $M_{c,\text{min}}/M_c = \sin i$ for randomly oriented orbits (solid line).

5 CONCLUSION

We have demonstrated that the relation between orbital period and companion white dwarf mass of recycled MSPs that have evolved via Case B RLOF is largely independent of initial donor mass, neutron star mass and how conservative is the mass transfer. It does however depend on the metallicity of the donor star because this changes the radius to core mass relation for red giants. For a companion of $1 M_\odot$, about the smallest that can be expected to evolve within the Galactic field, the lowest orbital period BMSPs formed without additional angular momentum loss have $P_{\text{orb}} \approx 6.2$ d. However with magnetic braking, or some alternative angular momentum loss mechanism, the relation can be extended down to $P_{\text{orb}} < 1$ d.

We selected all Galactic BMSPs, with $P_{\text{spin}} < 30$ ms, that could have been recycled by accretion from a red giant with a helium core that is now a He white dwarf companion from those listed in the ATNF catalogue. With our $P_{\text{orb}} - M_c$ relation we calculated the orbital inclinations of these systems, assuming a set of pulsar masses. We find that when the pulsar mass is taken to be as large as possible up to a maximum of $1.55 M_\odot$ the distribution of inclinations is consistent with random orientation of the orbits in space. If the maximum pulsar mass is reduced to $1.35 M_\odot$ there appears a dearth of high inclination systems and if it is raised to $1.75 M_\odot$ there appears an excess. Hence we deduce that all systems selected, and listed in Table A1 without bullets, are consistent with having pulsars of mass around $1.6 M_\odot$, having been recycled by accretion from a red giant with a helium core and having no observational bias towards particular orbital orientation. Given that selection of particular orbital inclinations would be encouraged if MSP magnetic axes and hence their beams were preferentially aligned with or orthogonal to their spin axes, our result is consistent with

random orientation of magnetic axes too. Numbers of systems remain too small to make conclusions about systems in different orbital period ranges.

ACKNOWLEDGEMENTS

SLS thanks STFC for her studentship. CAT thanks Churchill College for his fellowship. LF and DTW thank the Institute of Astronomy for supporting visits. SLS thanks Philip Hall for help in making detailed stellar models with mass transfer. We also thank the referee for many suggestions that have led to significant improvements to this work.

APPENDIX A: LIST OF SELECTED BMSPS

Table A1 lists all ATNF millisecond pulsars, with $P_{\text{spin}} < 30$ ms and $P_{\text{orb}} > 1$ d in the Galactic field. The fourth column lists the companion mass derived from our $P_{\text{orb}} - M_c$ relation. The fifth column is the measured mass function, reconstructed from the minimum mass given in the ATNF catalogue. The sixth column is the maximum neutron star mass that could be accommodated with the given mass function and derived companion mass. Systems in which $M_{\text{amax}} < 1.2 M_{\odot}$ are marked and excluded from further analysis. The final column indicates whether there is any determination of the companion's type.

REFERENCES

- Alexander D. R., Ferguson J. W., 1994, *ApJ*, 437, 879
 Alpar M. A., Cheng A. F., Ruderman M. A., Shaham J., 1982, *Nat*, 300, 728
 Angulo C. et al., 1999, *Nuclear Physics A*, 656, 3
 Antoniadis J., van Kerkwijk M. H., Koester D., Freire P. C. C., Wex N., Tauris T. M., Kramer M., Bassa C. G., 2012, *MNRAS*, 423, 3316
 Antoniadis J. et al., 2013, *Science*, 340, 448
 Backer D. C., 1998, *ApJ*, 493, 873
 Benvenuto O. G., De Vito M. A., 2003, *MNRAS*, 342, 50
 Böhm-Vitense E., 1958, *Z. Astrophys.*, 46, 108
 Buchler J. R., Yueh W. R., 1976, *ApJ*, 210, 440
 Burderi L., D'Antona F., di Salvo T., Lavagetto G., Iaria R., Robba N. R., 2005, in Rasio F. A., Stairs I. H., eds, *ASP Conf. Ser. Vol. 328, Binary Radio Pulsars*. Astron. Soc. Pac., San Francisco, p. 269
 Canuto V., 1970, *ApJ*, 159, 641
 Caughlan G. R., Fowler W. A., 1988, *Atomic Data and Nuclear Data Tables*, 40, 283
 Chen K., Ruderman M., Zhu T., 1998, *ApJ*, 493, 397
 Corongiu A. et al., 2012, *ApJ*, 760, 100
 Demorest P. B., Pennucci T., Ransom S. M., Roberts M. S. E., Hessels J. W. T., 2010, *Nat*, 467, 1081
 De Vito M. A., Benvenuto O. G., 2010, *MNRAS*, 401, 2552
 De Vito M. A., Benvenuto O. G., 2012, *MNRAS*, 421, 2206
 Eggleton P. P., 1971, *MNRAS*, 151, 351
 Fabian A. C., Pringle J. E., Verbunt F., Wade R. A., 1983, *Nat*, 301, 222
 Ferguson J. W., Alexander D. R., Allard F., Barman T., Bodnarik J. G., Hauschildt P. H., Heffner-Wong A., Tamanai A., 2005, *ApJ*, 623, 585
 Fruchter A. S., Gunn J. E., Lauer T. R., Dressler A., 1988, *Nat*, 334, 686
 Gonzalez M. E. et al., 2011, *ApJ*, 743, 102
 Han Z., Podsiadlowski P., Eggleton P. P., 1994, *MNRAS*, 270, 121
 Hubbard W. B., Lampe M., 1969, *ApJS*, 18, 297
 Hurley J. R., Tout C. A., Wickramasinghe D. T., Ferrario L., Kiel P. D., 2010, *MNRAS*, 402, 1437
 Iglesias C. A., Rogers F. J., 1996, *ApJ*, 464, 943
 Jacoby B. A., Hotan A. W., Bailes M., Ord S. M., Kulkarni S. R., 2005, *BAAS*, 37, 1468
 Jayawardhana R., Grindlay J. E., in Bailes M., Johnston S., Walker M. A., eds, *ASP Conf. Ser. Vol. 105, IAU Colloq. 160, Pulsars: Problems and Progress*. Astron. Soc. Pac., San Francisco, p. 231
 Kippenhahn R., Weigert A., 1967, *Z. Astrophys*, 65, 251
 Kippenhahn R., Weigert A., Hofmeister E., 1967, in Alder B., Fernbach S., Rothenberg M., eds, *Methods in Computational Physics Vol. 7*, Academia, New York, p. 129
 Konacki M., Wolszczan A., *ApJ*, 591, L147
 Lorimer D. R., 2008, *Living Rev. Relativ.*, 11, 8
 Manchester R. N., Hobbs G. B., Teoh A., Hobbs M., 2005, *AJ*, 129, 1993
 Nice D. J., Stairs I. H., Kasian L. E., 2008, in Bassa C., Wang Z., Cumming A., Kaspi V. M., eds, *Am. Inst. Phys. Conf. Ser. Vol. 983, 40 Years of Pulsars: Millisecond Pulsars, Magnetars and More*. p. 453
 Nomoto K., 1984, *ApJ*, 277, 791
 Papitto A. et al., 2013, *Nat*, 501, 517
 Paczyński B., 1971, *Acta Astron.*, 21, 417
 Podsiadlowski P., Rappaport S., Pfahl E. D., 2002, *ApJ*, 565, 1107
 Pols O. R., Schröder K.-P., Hurley J. R., Tout C. A., Eggleton P. P., 1998, *MNRAS*, 298, 525
 Pols O. R., Tout C. A., Eggleton P. P., Han Z., 1995, *MNRAS*, 274, 964
 Press W. H., Teukolsky S. A., Vetterling W. T., Flannery B. P., 1992, *Numerical Recipes in C. The Art of Scientific Computing*. Cambridge Univ. Press, Cambridge
 Radhakrishnan V., Srinivasan G., 1982, *Current Science*, 51, 1096
 Rappaport S., Podsiadlowski P., Joss P. C., Di Stefano R., Han Z., 1995, *MNRAS*, 273, 731
 Refsdal S., Weigert A., 1971, *A&A*, 13, 367
 Ruderman M., Chen K., 1999, in Arzoumanian Z., Van der Hooft F., van den Heuvel E. P. J., eds, *Pulsar Timing, General Relativity and the Internal Structure of Neutron Stars*. Koninklijke Nederlandse Akademie van Wetenschappen, Amsterdam, p. 223
 Schönberg M., Chandrasekhar S., 1942, *ApJ*, 96, 161
 Schröder K.-P., Pols O. R., Eggleton P. P., 1997, *MNRAS*, 285, 696
 Schwab J., Podsiadlowski P., Rappaport S., 2010, *ApJ*, 719, 722
 Shao Y., Li X.-D., 2012, *ApJ*, 756, 85
 Smith M. A., 1979, *PASP*, 91, 737
 Splaver E. M., 2004, PhD thesis, Princeton Univ.
 Splaver E. M., Nice D. J., Stairs I. H., Lommen A. N., Backer D. C., 2005, *ApJ*, 620, 405
 Stairs I. H. et al., 2005, *ApJ*, 632, 1060
 Stancliffe R. J., Eldridge J. J., 2009, *MNRAS*, 396, 1699
 Sugimoto D., Nomoto K., 1980, *Space Sci. Rev.*, 25, 155

Table A1. Binary millisecond pulsars in the ATNF Pulsar Catalogue in the Galactic field with $P_{\text{orb}} > 1$ d. Systems with superscript ^B were in the sample of Backer (1998) and those with a subscript _C have measured masses (see Table 1). The * symbols denote systems with minimum masses in the ATNF catalogue larger than $0.5 M_{\odot}$. The pulsar spin period is P_{spin} and P_{orb} is the orbital period. The companion mass M_c is computed from P_{orb} with our canonical relation. The measured mass function f is calculated from M_m given in the ATNF catalogue and $M_{\text{a,max}}$ is then the maximum pulsar mass that can be accommodated given f and M_c . The • symbols denote systems for which $M_{\text{a,max}} < 1.20 M_{\odot}$ and therefore do not fit the model. The final column lists any information on or suggestion of the type of the companion to be found in references given in the ATNF catalogue. MS = Main-sequence star, CO = CO or ONeMg white dwarf, He = He white dwarf, UL = Ultra-light companion or planet ($M_c < 0.08 M_{\odot}$) and U = undetermined companion type. A letter T at the end denotes that there are more than two components in the system. We excluded the systems with UL companions, MS companions and multiple systems. Many of the MSPs with thought to have CO companions have minimum masses in the ATNF catalogue larger than $0.5 M_{\odot}$. All are excluded because they require a minimum neutron star mass of less than $1.20 M_{\odot}$.

Name	$P_{\text{spin}}/\text{ms}$	P_{orb}/d	M_c/M_{\odot}	f/M_{\odot}	$M_{\text{a,max}}/M_{\odot}$	Comp. Type
J0613–0200 ^B	3.06184408653189	1.1985125753	0.187	0.00097185502	2.408	He
J1435–6100*	9.347972210248	1.3548852170	0.191	0.13832189	0.033•	CO
J2043+1711	2.37987896026	1.482290809	0.194	0.0020928803	1.675	He
J1909–3744 _C	2.9471080681076401	1.533449474590	0.195	0.0031219739	1.350	He
J0034–0534 ^B	1.8771818845850	1.589281801	0.197	0.0012634271	2.257	He
J1622–6617	23.62344473927	1.640635183	0.198	0.00037472931	4.346	U
J0101–6422	2.5731519721683	1.787596706	0.201	0.0016538449	2.008	He
J1231–1411	3.683878711077	1.860143882	0.202	0.0026445979	1.559	He
J1949+3106*	13.1381833437040	1.949535	0.203	0.10938610	0.073•	CO
J0218+4232 ^B	2.3230904678309	2.028846084	0.204	0.0020384352	1.832	He
J1439–5501*	28.634888190455	2.117942520	0.205	0.22759446	–0.011•	CO
J2017+0603	2.896215815562	2.198481129	0.205	0.0023426589	1.716	He
J2317+1439 ^B	3.4452510710225	2.459331464	0.208	0.0021994253	1.808	He
J1502–6752	26.7444237673	2.4844570	0.208	5.5708571e–06	39.908	UL
B1802–07	23.10085528430	2.61676335	0.209	0.0094491902	0.774•	U
J1911–1114 ^B	3.6257455713977	2.71655761	0.210	0.00079709848	3.196	He
J1431–5740	4.1105439567658	2.726855823	0.210	0.0016887826	2.131	U
J1748–3009	9.684273	2.9338198	0.212	0.00028695598	5.545	He
J1216–6410	3.539375658423	4.03672718	0.220	0.0016694467	2.300	He
J1045–4509 ^B	7.47422422621133	4.0835292547	0.220	0.0017649364	2.235	He
J1337–6423*	9.423406713	4.78533407	0.224	0.10508201	0.103•	CO
J1745–0952	19.3763034411294	4.943453386	0.225	0.00059126344	4.170	He
J1732–5049	5.31255028907845	5.262997206	0.226	0.0024490954	1.951	He
J0721–2038	15.54239497400	5.46083280	0.227	0.029704982	0.400•	U
J0437–4715 _C ^B	5.757451924362137	5.74104646	0.227	0.0012431183	2.835	He
J1545–4550	3.57528861884712	6.203064928	0.227	0.0015885663	2.480	U
J1811–2405	2.66059331690	6.27230204	0.227	0.0050692659	1.289	He
J1603–7202 ^B	14.84195224908935	6.3086296703	0.227	0.0087882681	0.925•	U
J1017–7156	2.3385144401138	6.5118988121	0.227	0.0028531163	1.800	He
J2129–5721 ^B	3.72634848296641	6.625493093	0.228	0.0010492057	3.123	He
J1835–0114	5.116387644239	6.6925427	0.228	0.0024171121	1.983	He
J2145–0750	16.05242391433660	6.83893	0.228	0.024105367	0.474•	CO
J1022+1001*	16.45292995078405	7.8051302826	0.233	0.083054673	0.157•	CO
J1543–5149	2.05696039242	8.06077304	0.234	0.0044968769	1.453	He
J0621+1002	28.853860730049	8.3186813	0.235	0.027026827	0.457•	CO
J1327–0755	2.6779231971205	8.439086019	0.235	0.0044251757	1.479	He
J1614–2230 _C	3.1508076534271	8.6866194196	0.236	0.020483367	0.565•	CO
J1125–6014	2.6303807397848	8.75260353	0.236	0.0081279214	1.036•	He
J1400–1438	3.0842332007	9.54743	0.238	0.0070342534	1.149•	He
J1841+0130	29.7727753332	10.471626	0.241	0.00042129066	5.523	He
J1918–0642	7.64587288390884	10.9131777486	0.242	0.0052494287	1.403	He
J1804–2717 ^B	9.343030685703	11.1287115	0.243	0.0033469189	1.825	He
B1855+09 _C ^B	5.362	12.32719	0.246	0.0055573963	1.389	He
J1900+0308	4.909239016418	12.47602144	0.246	0.0020899584	2.425	He
J2236–5527	6.907549392921	12.68918715	0.247	0.0045070041	1.578	U
J1933–6211	3.543431438847	12.81940650	0.247	0.012103419	0.869•	U
J1600–3053	3.59792850865547	14.3484577709	0.250	0.0035560324	1.851	He
J1741+1351	3.7471544	16.335	0.254	0.0053997280	1.491	He
J0900–3144	11.1096491573889	18.73763576	0.259	0.015693887	0.795•	U
J1801–3210	7.45358437341	20.7716995	0.263	0.0011851566	3.646	He
J1709+2313	4.6311962778409	22.71189238	0.265	0.0074382973	1.319	He
J1618–39	11.987313	22.8	0.265	0.0022177665	2.638	He
B1257+12	6.21853194840048	25.262	0.26856700	0.0000000	∞	UL

Table A1 – *continued* The binary millisecond pulsars in the ATNF Pulsar Catalogue that are in the galactic field.

Name	$P_{\text{spin}}/\text{ms}$	P_{orb}/d	M_c/M_{\odot}	f/M_{\odot}	$M_{\text{a,max}}/M_{\odot}$	Comp. Type
J1844+0115	4.185543936664	50.6458881	0.295	0.0011918677	4.341	He
J1825-0319	4.553527919736	52.6304992	0.296	0.0023624627	3.020	U
J0614-3329	3.148669579439	53.5846127	0.297	0.0078951142	1.523	He
J2033+1734	5.9489575348502	56.30779527	0.299	0.0027759932	2.799	He
J1910+1256 _C	4.98358394056511	58.466742029	0.300	0.0029628574	2.720	He
J1713+0747 _C ^B	4.570136525082782	67.8251298718	0.306	0.0078961829	1.595	He
J1455-3330 ^B	7.987204796261	76.1745676	0.310	0.0062715859	1.869	He
J1125-5825	3.1022139189504	76.4032169	0.310	0.0070010555	1.754	He
J2019+2425 ^B	3.93452408033124	76.51163479	0.310	0.010686460	1.361	He
J1737-0811	4.1750173128551	79.517379	0.312	0.00013803925	14.497	U
J1850+0124	3.559763768043	84.949858	0.314	0.0058483603	1.989	He
J1935+1726	4.200101791882	90.76389	0.317	0.0042604451	2.416	He
J2229+2643 ^B	2.9778192947556	93.0158934	0.318	0.00083949925	5.866	He
J1903+0327*	2.14991236434921	95.174118753	0.319	0.13955857	0.163 [•]	MST
J1751-2857	3.9148731963690	110.7464576	0.325	0.0030130429	3.051	He
J1853+1303 _C	4.09179738145616	115.65378643	0.327	0.0054396584	2.207	He
B1953+29 ^B	6.1331665102401	117.34909728	0.327	0.0024167741	3.485	He
J2302+4442	5.192324646411	125.935292	0.331	0.0092095292	1.650	U
J1643-1224 ^B	4.62164151699818	147.01739776	0.338	0.00078297226	6.671	He
J1708-3506	4.50515894826	149.13318	0.338	0.0018287070	4.261	He
J1640+2224 ^B	3.16331581791380	175.46066194	0.346	0.0059074572	2.302	He
B1620-26	11.0757509142025	191.44281	0.350	0.0079748112	1.972	HeT
J0407+1607	25.70173919463	669.0704	0.437	0.0028931881	4.939	He

Tauris T. M., Savonije G. J., 1999, A&A, 350, 928
Thorsett S. E., Chakrabarty D., 1999, ApJ, 512, 288
van Kerkwijk M. H., Bassa C. G., Jacoby B. A., Jonker P. G., 2005, in Rasio F. A., Stairs I. H., eds, ASP Conf. Ser. Vol. 328, Binary Radio Pulsars. Astron. Soc. Pac., San Francisco, p. 357
Verbiest J. P. W. et al., 2008, ApJ, 679, 675
Verbunt F., Zwaan C., 1981, A&A, 100, L7
Zhang C. M. et al., 2011, A&A, 527, A83